

Simultaneous adsorption of oxytetracycline and arsenic onto hydrous zirconium-modified chitosan/β-cyclodextrin composite: Mechanistic insights via statistical physics modeling, fractal-like kinetics, thermodynamic evaluation, and site energy distribution analysis

Mohd Nasir ^a, Sana ^a, Atif Afroz ^a Mohammad Kashif ^{a*} Abdul Malik ^b, Nikhat J Siddiqi ^c and Sara Aiman ^d

^a Analytical Chemistry Section, Department of Chemistry, Aligarh Muslim University, Aligarh-202002 (U.P.), India.

^b Department of Pharmaceutics, College of Pharmacy, King Saud University, Saudi Arabia, P.O. Box: 2455, 11451 Riyadh, Saudi Arabia.

^c Department of Internal Surgical Nursing, College of Nursing, King Saud University, Saudi Arabia, P.O. Box: 2455, 11451 Riyadh, Saudi Arabia.

^d Guangdong Provincial Key Laboratory of Medical Immunology and Molecular Diagnostics, The First Dongguan Affiliated Hospital, Guangdong Medical University, Dongguan, 523808, China

* mkashif25@gmail.com

Supplementary Information

Number of pages: 14

Number of tables: 8

Number of figures: 6

Table of Contents

Text S1: Characterization Techniques

The physiochemical properties of the synthesized hydrous zirconium-modified chitosan-β-cyclodextrin composite (Zr-CCS-g-β-CD) were systematically characterized using a suite of advanced analytical instruments. The pH of the working solutions was measured using a calibrated pH meter (Cyberscan pH 2100, Eutech Instruments) to ensure precise control of

experimental conditions. The quantification of the OCT and As (III) in aqueous solutions was carried out via UV-Visible spectrophotometry using a UV-1800 spectrophotometer (Shimadzu, Japan). The structural and functional group analysis of the material was performed by Fourier Transform Infrared (FT-IR) spectroscopy using a PerkinElmer Spectrum 2 spectrometer, recording spectra over the wavenumber range of 4000–400 cm^{-1} . The surface morphology and elemental composition of the composite were investigated by Scanning Electron Microscopy (SEM) coupled with Energy-Dispersive X-ray Spectroscopy (EDX) on a JEOL JSM-6510LV microscope (Japan). Specific surface area, pore size, and pore volume were evaluated through nitrogen gas adsorption-desorption isotherms at 77 K, obtained using a Micromeritics ASAP 2020 instrument. The crystallinity and phase purity of the material were determined by Powder X-ray Diffraction (PXRD) employing a Bruker AXS D8 Advance diffractometer (Germany) using $\text{Cu K}\alpha$ radiation ($\lambda = 0.154 \text{ nm}$). X-ray Photoelectron Spectroscopy (XPS) analysis was carried out on a Thermo Scientific K-Alpha spectrometer to investigate the surface elemental composition and chemical states of the material. The thermal stability and decomposition behavior were examined by simultaneous Thermogravimetric and Differential Thermal Analysis (TGA-DTA) using a DTG 60H thermal analyzer (Shimadzu, Japan). Furthermore, the hydrodynamic diameter and zeta potential of the composite particles were determined via Dynamic Light Scattering (DLS) and electrophoretic mobility measurements using a Horiba SZ-100 nanoparticle analyzer.

Text S2: Assessment of surface charge properties

To investigate the surface charge behavior of the Zr-CCS-g- β -CD composite, which plays a crucial role in the adsorption of oxytetracycline (OCT), the point of zero charge (pH_{pzc}) was determined using the salt addition method as described in the literature [51]. In this method, 100 mg of Zr-CCS-g- β -CD was added to a series of 100 mL conical flasks containing 50 mL of 0.01 M NaCl solution, with the initial pH (pH_i) adjusted from 2 to 12 using 0.15 M HCl or

0.15 M NaOH. The mixtures were stirred continuously for 48 hours at 298 K to reach equilibrium. After equilibration, the composite was separated by filtration, and the final pH (pH_f) of each solution was measured using a calibrated pH meter. The point of zero charge (pH_{pzc}) was identified by plotting the difference (Δ pH = pH_f – pH_i) against the initial pH. The pH at which Δ pH = 0 corresponds to the pH_{pzc}, indicating the surface charge neutrality of the composite, which directly influences the electrostatic interaction between Zr-CCS-g- β -CD and the ionizable forms of OCT under different pH conditions.

Text S3: Equilibrium adsorption isotherm studies

To investigate the equilibrium behavior of OCT adsorption onto the synthesized Zr-CCS-g- β -CD nanocomposite, a series of batch isotherm experiments were systematically conducted. Precisely 0.015 g of the adsorbent was accurately weighed and added to 100 mL Erlenmeyer flasks, each containing 25 mL of OCT solution with varying initial concentrations ranging from **30 to 150 mg/L**. The pH of the solutions was maintained at **6.5**, a condition optimized in preliminary studies to favor the interaction between OCT molecules and the functional sites of the nanocomposite. The adsorption process was carried out in a **thermostatically controlled water bath shaker** operated at **140 rpm**, ensuring consistent mixing and contact between the adsorbent and the solution. To explore the influence of temperature on the adsorption equilibrium, the experiments were conducted at four different temperatures: **298 K, 308 K, and 318 K**. The contact time for all isotherm studies was fixed at **45 minutes**, which was predetermined to be sufficient for attaining adsorption equilibrium under the given experimental conditions. Upon completion of each run, the mixture was filtered to remove the solid adsorbent, and the **residual concentration of OCT** in the filtrate was quantified spectrophotometrically by measuring the absorbance at **228 nm** using a calibrated UV-VIS spectrophotometer. The equilibrium adsorption capacity (q_e , mg g⁻¹) of the adsorbent was calculated using the following expression:

$$q_e = \frac{(C_i - C_f)V}{M} \quad (S1)$$

M and V are mass (g) of the Zr-CCS-g- β -CD and volume of the solution in liter (L), respectively.

Text S4: Adsorption Kinetic Studies

The kinetic behavior governing the adsorption of OCT onto Zr-CCS-g- β -CD was systematically investigated under controlled batch conditions. For this purpose, a predetermined mass of Zr-CCS-g- β -CD (0.015 g) was dispersed in 25 mL of OCT solution with an initial concentration of 30 mg/L, adjusted to pH 6.0. The suspensions were transferred into a series of 100 mL Erlenmeyer flasks and subjected to constant agitation at 140 rpm in a thermostatically regulated water bath shaker. The experiments were conducted at four distinct temperatures (298, 303, 308, and 313 K) to evaluate the temperature dependence of the adsorption kinetics. At predetermined time intervals (5, 10, 30, 60, 90, 120, 180, and 240 minutes), individual flasks were withdrawn from the shaker, and the adsorbent was separated from the solution via filtration. The residual concentration of OCT in the supernatant was quantified by UV-Visible spectrophotometry at 228 nm. The amount of OCT adsorbed onto the Zr-CCS-g- β -CD at each contact time (q_t , mg/g) was calculated using Eq (S2):

$$q_t = \frac{(C_o - C_t)V}{M} \quad (S2)$$

where C_o and C_t are the concentration of OCT at time zero and t , respectively. The obtained kinetic data were subsequently fitted to various kinetic models, including pseudo-first-order, pseudo-second-order, Elovich, intraparticle diffusion, and fractal-like kinetic models, to elucidate the underlying adsorption mechanisms and rate-controlling steps.

Text S5: Regeneration and reusability assessment

The desorption and reusability performance of Zr-CCS-g- β -CD was systematically evaluated through multiple adsorption–desorption cycles to assess the material’s stability and economic feasibility for repetitive use in OCT removal. For each desorption cycle, 0.015 g of OCT-saturated Zr-CCS-g- β -CD was immersed in 25 mL of 0.010 M hydrochloric acid (HCl) solution and subjected to continuous agitation for 60 minutes, facilitating the protonation of functional groups and promoting the release of adsorbed OCT molecules from the sorbent surface. After desorption, the mixture was filtered to recover the solid phase, and the OCT concentration in the filtrate was determined spectrophotometrically at 228 nm. The recovered Zr-CCS-g- β -CD were subsequently regenerated by treating the material with 25 mL of 0.15 M sodium hydroxide (NaOH) solution, aiming to neutralize and restore the surface charge of the functional groups. This was followed by extensive rinsing with demineralized water until a neutral pH was achieved, to ensure the complete removal of any residual desorbing agent. The regenerated adsorbent was then dried in a hot air oven at an appropriate temperature to eliminate any moisture content before being reused in the next adsorption cycle. This adsorption–desorption–regeneration process was repeated for a total of seven consecutive cycles under identical conditions. The adsorption efficiency after each cycle was monitored to evaluate the structural robustness and reusability of Zr-CCS-g- β -CD, thus offering insight into its potential for practical applications in sustainable wastewater treatment systems.

Equations

$$\chi^2 = \frac{\sum_{i=1}^n (q_{e,exp} - q_{e,cal})^2}{q_{e,exp}} \quad (S3)$$

$$RMSE = \sqrt{\frac{1}{n} \sum_{i=1}^n (q_{e,cal} - q_{e,exp})^2} \quad (S4)$$

Table S1 Independent variables and their levels used for central composite design.

Variables	Unit	Factor	Range and level				
			- α	-1	0	+1	+α
Adsorbent dosage	(g)	A	0.0086	0.010	0.012	0.014	0.0154
Initial concentration	(mg/L)	B	5.91	40.00	90.00	140.00	174.09
Contact time	(min.)	C	6.36	20.00	40.00	60.00	73.64

Table S2 Mathematical expressions of classical isotherm statistical physics models and its parameters

Classical isotherm	Non-linear equation	Parameters
Langmuir	$q_e = \frac{q_m K_L C_e}{1 + K_L C_e}$	q_m, K_L and C_e
Freundlich	$q_e = K_F C_e^{1/n}$	K_F and n
Statistical physics models		
Model 1 (M₁)	$q_e = n N_o \frac{n N_m}{1 + \left(\frac{C_{1/2}}{C_e}\right)^n} = \frac{Q_{sat}}{1 + \left(\frac{C_{1/2}}{C_e}\right)^n}$	n, N_o and N_m

Model 2 (M₂)	$q_e = \frac{n_1 \cdot N_{m1}}{1 + \left(\frac{C_1}{C}\right)^{n_1}} + \frac{n_2 \cdot N_{m2}}{1 + \left(\frac{C_2}{C}\right)^{n_2}}$	n_1, n_2, N_{m1} and N_{m2}
Model 3 (M₃)	$q_e = n \cdot N_m \left(\frac{\left(\frac{C}{C_{1/2}}\right)^n + 2\left(\frac{C}{C_{1/2}}\right)^{2n}}{1 + \left(\frac{C}{C_{1/2}}\right)^n + \left(\frac{C}{C_{1/2}}\right)^{2n}} \right)$	n and N_m
Model 4 (M₄)	$q_e = n \cdot N_m \left(\frac{\left(\frac{C}{C_1}\right)^n + 2\left(\frac{C}{C_1}\right)^{2n}}{1 + \left(\frac{C}{C_1}\right)^n + \left(\frac{C}{C_2}\right)^{2n}} \right)$	n and N_m

where q_e : experimental adsorption capacity (mg/g), q_m : calculated adsorption capacity (mg/g),

C_e : concentration of cloxacillin in the solution phase at equilibrium(mg/L), k_L : Langmuir

$\frac{1}{k_F \cdot n}$ isotherm constant (L/mg), k_F & n are Freundlich isotherm constants. N_m and n are the density of adsorption sites, occupied by adsorbate (mg/g) and number species which are adsorbed, respectively. $C_{1/2}$ and C are the concentration of acetaminophen (mg/L) at half saturation and equilibrium concentration (mg/L), respectively. C_1 and C_2 suggested the concentration (mg/L) at half saturation of first and second adsorption sites, respectively. N_{m1} and N_{m2} are the density of first and second adsorption sites, respectively. n_1 and n_2 indicate the number of adsorbed species at first and second adsorption sites, respectively

Table S3 Nonlinear Langmuir and Freundlich isotherm parameters and error values

Isotherm	Temp. (K)	Parameters (Linear)			Error Functions		
		q_{m^*} (mg/g)	K_L (L/mg)	R^2	RMSE	χ^2	
	298	171.47	0.587	0.9784	29.86	1.37	

Langmuir	308	219.04	0.279	0.8973	29.35	1.798
	318	254.35	0.973	0.8895	38.96	9.875
		q _{m*} (mg/g)	n	K _F		
	298	187.20	3.657	53.92	0.9997	0.3200
Freundlich	308	199.91	3.278	49.59	0.9995	0.1600
	318	208.28	2.992	46.28	0.9995	0.6500

* The experimental values of adsorption capacity (q_e) for acetaminophen are 187.52 mg/g, 200.07 and 208.93 mg/g at 298, 308 and 318 K, respectively.

Table S4 Mathematical expressions of statistical physics models with R^2 and SSE for fitting of experimental date for the adsorption of acetaminophen onto

Models	Temp (K)	Parameters		
		R^2	χ^2	RMSE
Model 1 (M₁)	298	0.9897	1.97	18.33
	308	0.8802	1.93	17.38
	318	0.8943	5.141	21.52
Model 2 (M₂)	298	0.9996	0.0058	0.997
	308	0.9998	0.0079	1.059
	318	0.9997	0.0099	1.086
Model 3 (M₃)	298	0.8952	2.58	30.27
	308	0.9698	2.37	30.012
	318	0.9802	3.371	20.738
Model 4 (M₄)	298	0.8891	3.57	20.723
	308	0.9492	3.69	20.835
	318	0.8997	7.2337	32.395

*The experimental values of adsorption capacity (q_e) for acetaminophen are 187.52 mg/g, 200.07 and 208.93 mg/g at 298, 308 and 318 K, respectively.

Table S5 The fitting results for the M₂ model

Parameters	Temperature		
	298 K	308 K	318 K
N _m	0.643	0.659	0.671
N	0.832	0.792	0.7417
a ₁	0.4056	0.4438	0.4672
a ₁	1.669	1.627	1.155

Table S6 Mathematical expression for the surface-based kinetics (Classical and fractal models) diffusion base kinetic model.

Surface based kinetic studies (Classical models)	Mathematical expression
PFO	$q_t = q_e \left(1 - e^{-k_1 t}\right)$
PSO	$q_t = \frac{q_e^2 k_2 t}{1 + q_e k_2 t}$
Surface based kinetic studies (fractal-like kinetic models)	Mathematical expression
F-L PFO	$q_t = q_e \left[1 - \exp(-k_{1,0} t^\alpha)\right]$
F-L PSO	$q_t = \frac{k_{2,0} q_e^2 t^\alpha}{1 + k_{2,0} q_e t^\alpha}$
Diffusion based kinetic model	
Intraparticle diffusion model	$q_t = k_{id} t^{1/2} + C_{id}$

In these equations $k_{1,0}$ ($1/min^\alpha$) and $k_{2,0}$ ($mg/g/min^\alpha$) express the rate coefficients of Fractal-like-PFO, Fractal-like-PSO, respectively. α denotes fractional time index which is

defined as $\alpha = (1 - h)$. k_{id} (mg/g min^{-0.5}) and C_{id} (mg/g) denotes the intraparticle diffusion rate constant and the boundary layer effect, respectively.

Table S7 Classical and fractal-like kinetic parameters and regression coefficients obtained by nonlinear regression analysis for the uptake of OCT onto Zr-CCS-g- β -CD.

Surface based kinetic model (Classical model)	Parameters	Temperature		
		298 K	308 K	318 K
PFO	q_m (mg/g)	62.351	66.619	68.096
	K_1 (1/min)	0.0429	0.0637	0.0522
	R^2	0.889	0.908	0.965
	χ^2	1.483	2.709	5.244
	RMSE	9.620	13.43	18.89
PSO	q_m (mg/g)	71.025	79.593	86.594
	K_2 (g/mg/min)	0.006	0.009	0.016
	R^2	0.9992	0.9998	0.9999
	χ^2	0.0125	0.00265	0.00192
	RMSE	0.943	0.459	0.408
(Fractal Model)				
FL-PFO	q_m (mg/g)	67.278	70.082	78.161
	$k'_{1,0}$ (1/min ^(1-h))	0.183	0.149	0.115
	α	0.822	0.798	0.706
	R^2	0.9798	0.9893	0.9695
	χ^2	0.327	1.418	1.000
	RMSE	4.69	9.97	8.84

FL-PSO	q_m (mg/g)	72.453	80.936	87.246
	$k'_{2,0}$ (g/mg/min ^(1-h))	0.0092	0.0012	0.0019
	α	0.991	0.627	0.583
	R^2	0.9996	0.9999	0.9998
	χ^2	0.00324	0.00965	0.00068
	RMSE	0.485	0.884	0.244

($q_{e,exp}$: 71.968, 80.052 and 87.002 mg/g at 298, 308 and 318 K, respectively. Experimental conditions: initial concentration = 50 mg/L, pH = 6.5, contact time = 45 min, adsorbent dosage = 0.01 g).

Table S8 Diffusion based kinetic parameters and regression coefficients obtained by linear regression analysis for the adsorption of PCM onto ZnO/Cs-In.

Kinetic model	Parameters	Temperature (K)		
		298	308	318
I	C_{id}	32.53	37.077	36.306
	K_{id} (mg/g.min ^{1/2})	6.812	6.7000	8.1143
	R^2	0.9998	0.9997	0.9984
Intra-particle diffusion model	C_{id}	64.171	66.138	74.396
	K_{id} (mg/g.min ^{1/2})	1.0131	1.3649	1.0672
	R^2	0.9895	0.9977	0.9614

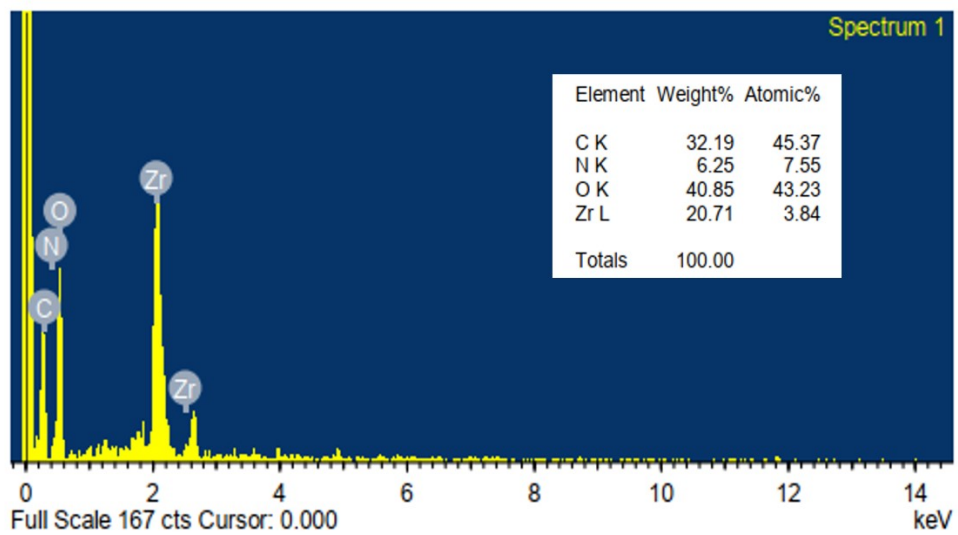


Fig. S1 EDX spectrum of Zr-CCS-g- β -CD

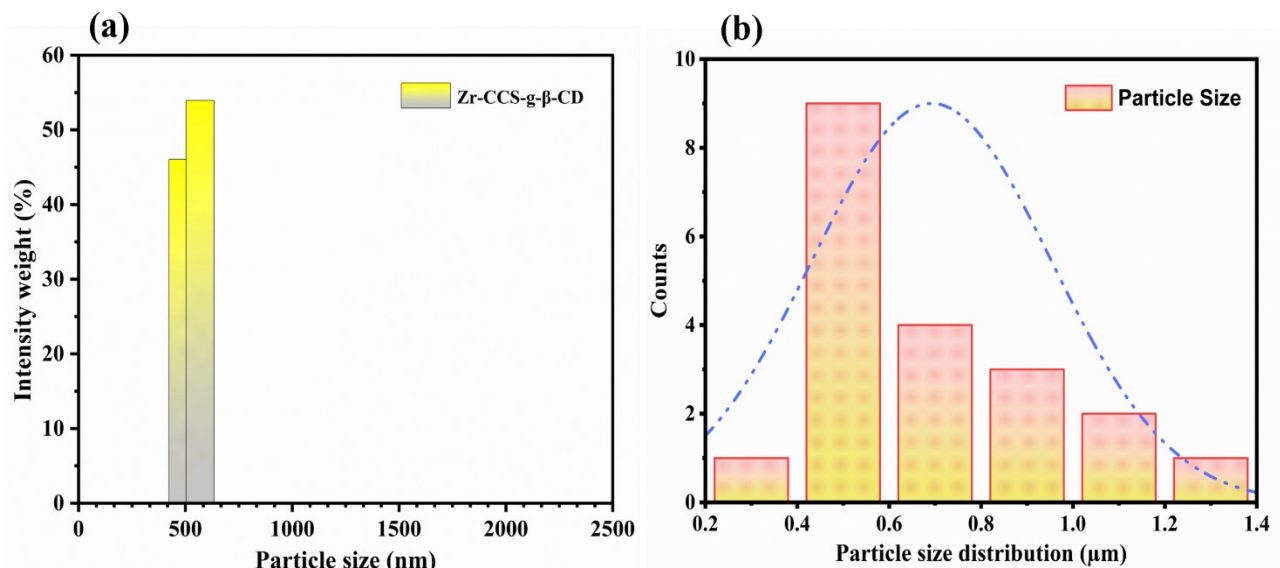


Fig. S2 Particle size distribution curve obtained through (a) dynamic light scattering (DLS) analysis and (b) scanning electron microscopy (SEM)

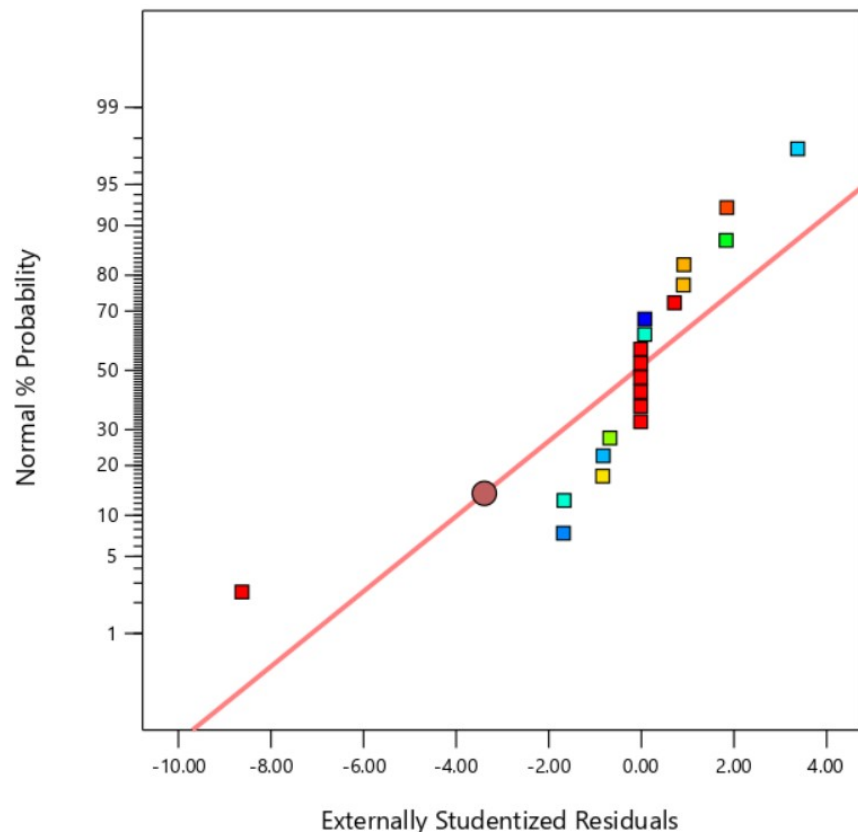


Fig. S3 Normal probability plot of externally studentized residuals for the fitted model

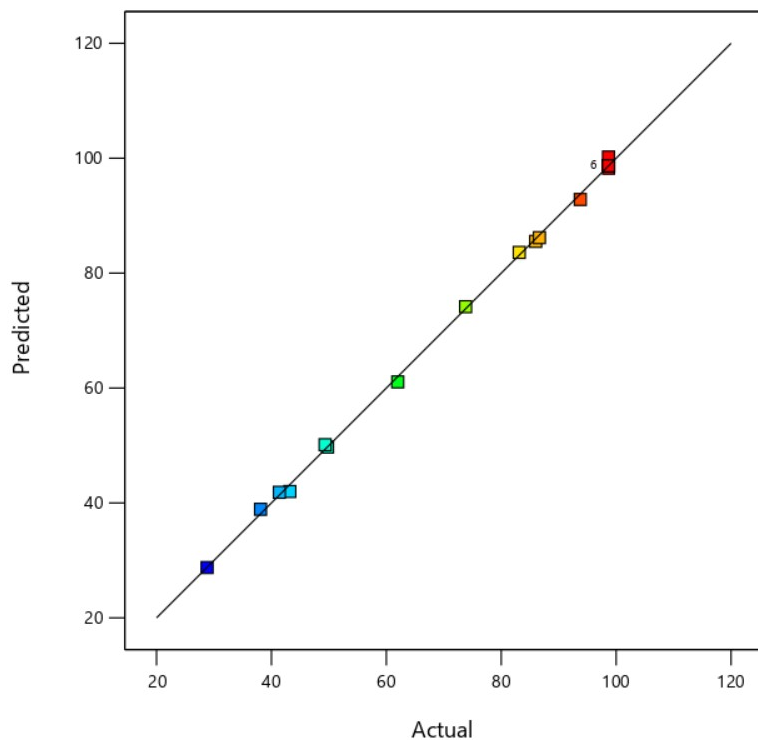


Fig. S4 Plot of predicted versus actual values for the developed mode.

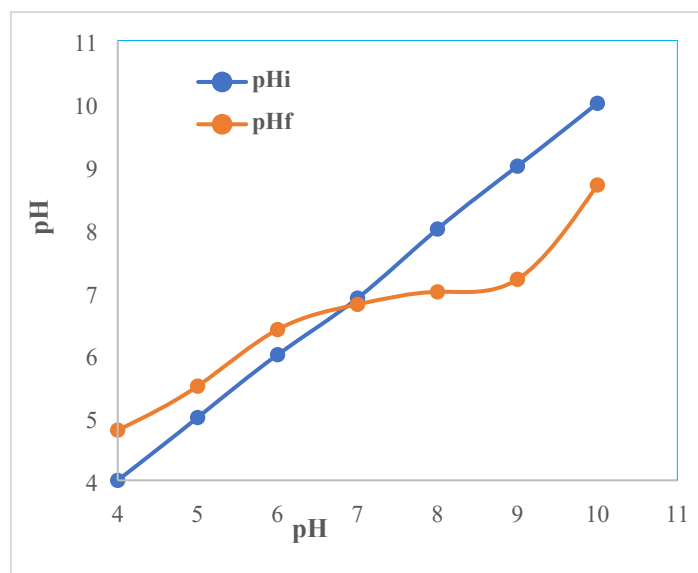


Fig. S5 Point of zero charge pH_{pzc} of the Zr-CCS-g- β -CD, determined by the pH drift method.

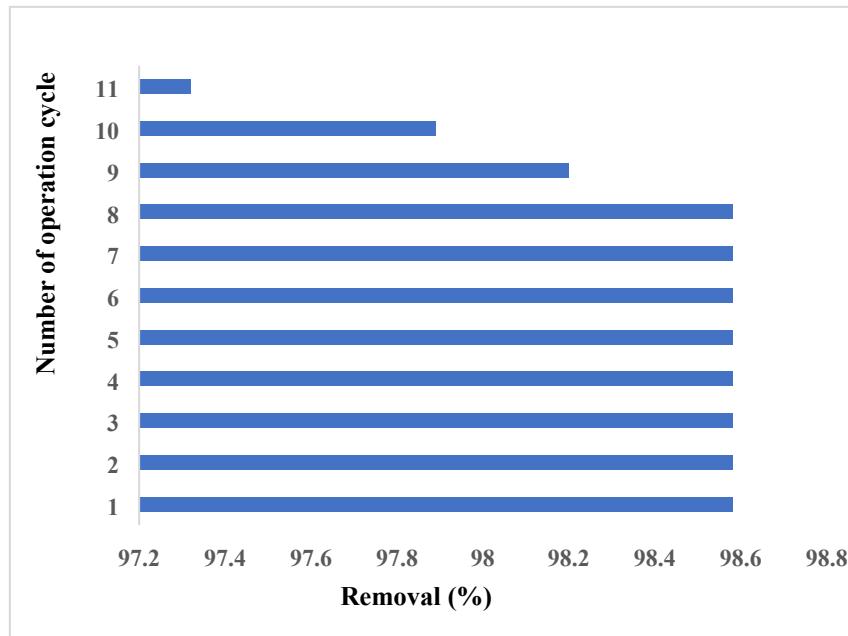


Fig. S6 Reuse and regeneration studies of Zr-CCS-g- β -CD nanocomposite